



Title	Membrane Protein Rim21 Plays a Central Role in Sensing Ambient pH in <i>Saccharomyces cerevisiae</i>
Author(s)	Obara, Keisuke; Yamamoto, Hayashi; Kihara, Akio
Citation	Journal of Biological Chemistry, 287(46), 38473-38481 <a href="https://doi.org/10.1074/jbc.M112.394205">https://doi.org/10.1074/jbc.M112.394205</a>
Issue Date	2012-11-09
Doc URL	<a href="http://hdl.handle.net/2115/51041">http://hdl.handle.net/2115/51041</a>
Rights	This research was originally published in Journal of Biological Chemistry. Keisuke Obara, Hayashi Yamamoto and Akio Kihara. Membrane Protein Rim21 Plays a Central Role in Sensing Ambient pH in <i>Saccharomyces cerevisiae</i> . Journal of Biological Chemistry. 2012; 287:38473-38481. © the American Society for Biochemistry and Molecular Biology.
Type	article (author version)
Additional Information	There are other files related to this item in HUSCAP. Check the above URL.
File Information	JBC287-46_38473-38481.pdf



[Instructions for use](#)

Membrane Protein Rim21 Plays a Central Role in Sensing Ambient pH in *Saccharomyces Cerevisiae*\*

Keisuke Obara<sup>1</sup>, Hayashi Yamamoto<sup>2</sup>, and Akio Kihara<sup>1</sup>

<sup>1</sup>From the Faculty of Pharmaceutical Sciences, Hokkaido University, Sapporo 062-0812, Japan

<sup>2</sup>Frontier Research Center, Tokyo Institute of Technology, Yokohama 226-8503, Japan

\*Running title: *Rim21 is the sensor protein that detects ambient pH*

To whom correspondence should be addressed: Akio Kihara, Faculty of Pharmaceutical Sciences, Hokkaido University, Kita 12-jo Nishi 6-chome, Kita-ku, Sapporo 060-0812, Japan, Tel.: +81-11-706-3754; Fax: +81-11-706-4900; E-mail: kihara@pharm.hokudai.ac.jp

**Keywords:** pH sensing; lipid; lipid asymmetry; Rim101 pathway

---

**Background:** Rim21, Dfg16, and Rim9 are considered to form a pH-sensor machinery in yeast.

**Results:** Transient degradation of Rim21 abolished pH sensing, while that of Dfg16 and Rim9 did not.

**Conclusion:** Rim21 is the sensor protein that detects ambient pH.

**Significance:** Elucidating the ambient pH-sensing mechanism is essential for understanding the adaptation of fungi, including fungal pathogens, to their local environment.

## SUMMARY

External alkalization activates the Rim101 pathway in *Saccharomyces cerevisiae*. In this pathway, three integral membrane proteins Rim21, Dfg16, and Rim9 are considered to be the components of the pH-sensor machinery. However, how these proteins are involved in pH sensing is totally unknown. In this work, we investigated the localization, physical interaction, and interrelationship of Rim21, Dfg16, and Rim9. These proteins were found to form a complex and to localize to the plasma membrane in a patchy and mutually-dependent manner. Their cellular level was also mutually dependent. In particular, the Rim21 level was significantly decreased in *dfg16Δ* and *rim9Δ* cells. Upon external alkalization, the proteins were internalized and degraded. We also demonstrated that the transient degradation of Rim21 completely suppressed the Rim101 pathway but the degradation of neither Dfg16 nor Rim9 did. This finding strongly suggests that Rim21 is the pH-sensor protein and that Dfg16 and Rim9 play auxiliary functions through

maintaining the Rim21 level and assisting its plasma membrane localization. Even without external alkalization, the Rim101 pathway was activated in a Rim21-dependent manner by either protonophore treatment or depletion of phosphatidylserine in the inner leaflet of the plasma membrane, both of which cause plasma membrane depolarization like the external alkalization. Therefore, the plasma membrane depolarization seems to be one of the key signals for the pH-sensor molecule Rim21.

---

Microorganisms that grow over a wide pH range, such as the yeast *Saccharomyces cerevisiae* and the filamentous fungi *Aspergillus nidulans*, must be capable of sensing and responding properly to changes in their ambient pH (1, 2). The adaptation to ambient pH is critical not only for survival but also for the pathogenicity of both animal and plant pathogens (3). Thus, the understanding of such adaptation mechanism is important for a broad range of sciences including biological, medical, and agricultural sciences.

External pH regulates expression of genes encoding secreted enzymes, permeases, and proteins involved in intracellular pH homeostasis (4-7). In yeast, the Rim101 pathway is known to mediate its adaptation to an alkaline environment, leading to expression of alkaline-responsive genes (2). Upon stimulation of this pathway, a transcription factor Rim101 undergoes proteolytic activation by a calpain-like protease Rim13. The activated Rim101 induces alkaline-responsive genes indirectly through repressing expression of transcription repressors such as Nrg1 and Smp1 (5, 6). Besides Rim13, three

integral membrane proteins Rim21, Dfg16, and Rim9 are essential for the Rim101 pathway (8-10). Epistatic analysis suggested that these proteins act in the most upstream of this pathway, probably sensing external alkalization (11). An arrestin-like protein Rim8 is also an essential component. Arrestin-like proteins are often involved in internalization of plasma membrane receptors and transporters *via* endocytosis (12, 13), although the involvement of endocytosis in the Rim101 pathway is currently under debate. In addition to these proteins, several endosomal sorting complex required for transport (ESCRT) proteins are necessary for the Rim101 pathway. ESCRT proteins, originally reported as proteins required for vacuolar protein sorting, function as subunits of large complexes (ESCRT-0, -I, -II, and -III) that are recruited in a sequential manner onto the surface of the endosome (14). Of them, ESCRT-I subunits Stp22/Vps23 and Vps28, ESCRT-II subunits Snf8/Vps22, Vps25, and Vps36, and ESCRT-III subunits Snf7 and Vps20 are shown to be required for the Rim101 pathway (15). It is reported that the Rim101 pathway is constitutively activated in *did4Δ*, *vps24Δ*, and *vps4Δ* mutants (11). These mutants lack Did4, Vps24, and Vps4, which are involved in the disassembly of ESCRT-III complex, thus accumulating the Snf7-Vps20 subcomplex of ESCRT-III on the endosome (16). Comprehensive analysis of protein interaction suggested that Snf7 interacts with Rim20, which binds to Rim101 (17, 18), as well as with Rim13 (17, 19). Based on these findings, it is proposed that Rim101 is proteolytically cleaved by Rim13 in a large complex comprised of Rim20, Snf7-Vps20, and Rim13 (11, 18).

In contrary to the proteolytic activation process of Rim101, the pH-sensing mechanism is mostly unknown. The integral membrane proteins Rim21, Dfg16, and Rim9 are thought to be potential sensor molecules, although their functional information is quite limited. Their biochemical information has also not been reported, including their cellular level, intracellular localization, post-translational modification, interrelationship, as well as their fate upon external alkalization. In *A. nidulans*, an integral membrane protein PalH is considered to be a pH-sensor molecule (20, 21). PalH predominantly localizes to the plasma membrane when co-overexpressed with another membrane protein PalI, the *A. nidulans* counterpart of Rim9, suggesting that PalI assists plasma membrane localization of PalH (22). Rim21 and Dfg16 are possible candidates for the yeast counterpart of PalH.

However, their sequence homologies with PalH are relatively low (27% for Rim21 and 19% for Dfg16) and, hence, their functional role is still elusive.

Recently, we reported that the Rim101 pathway senses altered lipid asymmetry in the plasma membrane as well as external alkalization (23). Like the pH-sensing mechanism, the lipid asymmetry-sensing mechanism is also unknown. To gain insight into both sensing mechanisms, biochemical characterization of the putative sensor proteins Rim21, Dfg16, and Rim9 is of at most importance. In this work, we have demonstrated that these proteins form a complex and localize to the plasma membrane in a patchy and mutually dependent manner. Using a transient protein degradation system, we have identified that Rim21 is the pH-sensor protein and that Dfg16 and Rim9 play auxiliary roles through maintaining Rim21 level and, presumably, through assisting its plasma membrane localization. Furthermore, we have demonstrated that plasma membrane depolarization stimulates the Rim101 pathway through Rim21 even without external alkalization.

## EXPERIMENTAL PROCEDURES

*Yeast strains and media*—*Saccharomyces cerevisiae* strains used in this study are listed in Table 1. Yeast cells were grown at 30 °C to log phase in either YPD medium (1% yeast extract, 2% peptone, and 2% D-glucose) or synthetic dextrose (SD) medium (2% D-glucose and 0.67% yeast nitrogen base without amino acids) with the appropriate supplements. The alkaline treatment was performed by adding 1 M Tris-HCl (pH 8.0) to the medium at the final concentration of 100 mM. A 500 mM stock solution of 3-indoleacetic acid (IAA, Nacalai Tesque, Kyoto, Japan) was prepared in ethanol and added to the medium at the final concentration of 500 μM. Since the conversion of phosphatidylserine (PS) to phosphatidylethanolamine (PE) is the major pathway for PE synthesis in yeast, the *CHO1*-deleted cells that lack PS show a significant reduction of PE, thus inviable in SD medium (24). Therefore, KCY1113 (*cho1Δ*) cells were grown in SD medium with the appropriate supplements and 1 mM ethanolamine, the precursor in an alternative pathway to PE. A 5 mM stock solution of carbonyl cyanide *m*-chlorophenylhydrazone (CCCP) was prepared in ethanol. For the CCCP treatment, cells were grown to log phase in SD medium with the appropriate supplements at pH 5.5 (buffered with 50 mM sodium citrate-HCl), and CCCP was added to the medium at the final concentration of 10 μM.

*Genetic manipulation*– Gene disruption was performed by replacing the entire coding region of the gene with a marker gene. Chromosomal fusion of HA, FLAG, GFP, 2xGFP, mCherry, HA-AID, and FLAG-AID to the C-terminus was performed using PCR-based gene disruption and modification (25). The sequence encoding a respective tag, the *ADH1* termination sequence, and a marker sequence (*KanMX6* or *TRP1*) was amplified by PCR from a pFA6a vector series (25) with a primer set containing the homologous region of the target gene. Amplified cassettes were inserted directly into the chromosome by homologous recombination.

*Plasmid construction*– To construct plasmids for the expression of Rim21-HA in yeast cells, the promoter region of *RIM21*, the *RIM21* coding sequence, the HA sequence, and the 3' UTR of *RIM21* were cloned in tandem into pRS313 and pRS423 (26) to generate pOK313 and pOK315, respectively. A linker sequence (two repeats of the sequence encoding GGS) was added before the coding sequence for HA. A multicopy plasmid overexpressing Rim21-FLAG (pOK311) was constructed in the same manner, except that the FLAG sequence was cloned instead of the HA sequence. To construct a multicopy plasmid overexpressing Rim21-HA and carrying the *TRP1* marker, the *PvuII* fragment derived from pOK313 was ligated into the *PvuII* site of pRS424 to yield pOK328. The plasmid encoding Dfg16-HA (pOK314) was constructed in the same manner as the pOK313 plasmid. To construct a multicopy plasmid overexpressing Dfg16-FLAG, the promoter region of *DFG16*, the *DFG16* coding sequence, and the FLAG sequence were cloned in tandem into pRS424 to generate pOK330. To construct Rim9-HA plasmids, the promoter region of *RIM9*, the *RIM9* coding sequence, and the HA sequence were cloned in tandem into pRS313 and pRS423 to generate pOK318 and pOK320, respectively. The *SUC2-RIM21-FLAG* plasmid was constructed as follows. The *BamHI* site was introduced after the start codon of *RIM21* in pOK311 using QuikChange site-directed mutagenesis kit (Stratagene, La Jolla, CA) to produce pOK377. The *SUC2* sequence was amplified by PCR from pSH69 (27) to have *BamHI* sites at both 5' and 3' ends, and cloned into the *BamHI* site of pOK377 to generate pOK387. The plasmid for the expression of Rim21-HA lacking the C-terminal region was constructed as follows. The promoter region of *RIM21* with a part of *RIM21*

coding sequence (1-1362) was amplified from yeast genomic DNA to have a linker sequence (two repeats of the sequence encoding GGS) after 1362. The promoter region and coding sequence of *RIM21* was excised from pOK313, and the amplified PCR fragment was instead cloned into the same site to generate pOK419. The plasmid for the expression of HA-Rim101 (pFI1) (11) was a kind gift from Dr. T. Maeda (University of Tokyo, Japan).

*Dephosphorylation and deglycosylation*– Cell lysates were prepared by alkaline-TCA method as described previously (28), except in  $\lambda$ -protein phosphatase ( $\lambda$ -PPase) buffer (1x  $\lambda$ -PPase buffer and 1x MnCl<sub>2</sub> solution, New England BioLabs, Beverly, MA) supplemented with 1 mM phenylmethylsulphonyl fluoride (PMSF). Each lysate was divided into two halves, and  $\lambda$ -PPase (New England BioLabs) was added to one of them to the final concentration of 20 units/ $\mu$ L. The lysate with or without  $\lambda$ -PPase was incubated at 30°C for 40 min with occasional mixing by tapping. Subsequently, a 1/3 volume of 4x SDS sample buffer was added and the mixture was incubated for an additional 10 min at 37°C. After dilution with a 4x volume of endoglycosidase H (Endo H) buffer (62.5 mM sodium citrate, pH 5.5, and 1.25 mM PMSF), Endo H (Endo Hf, New England BioLabs) was added to the final concentration of 20 units/ $\mu$ L and the mixture was incubated at 37°C for 1 hr with occasional mixing by tapping. The lysate was then treated with an appropriate volume of 4x SDS sample buffer at 37°C for 10 min.

*Immunoblot analysis*– Proteins were separated by SDS-PAGE and transferred to Immobilon<sup>TM</sup> polyvinylidene difluoride membrane (Millipore, Billerica, MA) as described previously (29). The membrane was incubated with anti-FLAG (M2, Stratagene), anti-HA (Y-11, Santa Cruz Biotechnology, Santa Cruz, CA; 16B12, Covance, Princeton, NJ; or 3F10, Roche Diagnostics, Indianapolis, IN), or anti-Pgk1 (Molecular Probes, Eugene, OR) antibody. Immunodetection was performed using ECL plus (GE Healthcare Biosciences, Piscataway, NJ) or Western Lightning ECL Pro system (PerkinElmer Life Sciences, Waltham, MA) with a bioimaging analyzer (LAS4000, Fuji Photo Film, Tokyo, Japan) or X-ray films. Can Get Signal Immunoreaction Enhancer Solution (TOYOBO, Osaka, Japan) was used for the Y-11 anti-HA antibody.

**Co-immunoprecipitation**– Cells with or without 5-min alkaline treatment were broken by mixing vigorously with glass beads at 4°C for 10 min using lysis buffer [50 mM Hepes-NaOH, pH 8.0 for alkaline-treated cells and pH 6.8 for non-treated cells, 150 mM NaCl, 5 mM MgCl<sub>2</sub>, 1 mM dithiothreitol, 1 mM PMSF, EDTA-free protease inhibitor cocktail (Complete, Roche Diagnostics)]. The cell lysate was sonicated and centrifuged at 1,000x g for 5 min to remove debris prior to the treatment with 1% Triton X-100 and 1% digitonin at 4°C for 1 hr. The mixture was then centrifuged at 100,000x g for 30 min, and the supernatant was incubated with anti-FLAG M2 agarose (Sigma, St. Louis, MO) while rotating at 4°C for 2 hr. The beads were washed three times with lysis buffer containing 0.1% Triton X-100 and 0.1% digitonin. The bound proteins were eluted with SDS sample buffer and separated by SDS-PAGE.

**Microscopy**– The intracellular localization of GFP- and mCherry-tagged proteins was observed using an inverted fluorescence microscope (IX-81, Olympus, Tokyo, Japan) equipped with an electron-multiplying CCD camera (ImageEM, C9100-13, Hamamatsu Photonics, Hamamatsu, Japan). For the simultaneous observation of GFP- and mCherry-fusion proteins, cells were excited simultaneously with blue (20 mW, Spectra-Physics, Santa Clara, CA) and yellow (25 mW, Cobalt Laser, Orlando, FL) lasers. Fluorescence was filtered with a Di01-R488/561-25 dichroic mirror (Semrock, Rochester, New York) and an Em01-R488/568-25 bandpass filter (Semrock), and separated into two channels using a U-SIP splitter (Olympus) equipped with a DM565HQ dichroic mirror (Olympus). The fluorescence was further filtered with an FF02-525/50-25 bandpass filter (Semrock) to analyze GFP and an FF01-624/40-25 bandpass filter (Semrock) to analyze mCherry.

## RESULTS

***Rim21, Dfg16, and Rim9 affect mutually their protein levels and phosphorylation status***– First, we investigated the post-translational modification and cellular level of Rim21, Dfg16, and Rim9 by immunoblot analysis of expressed HA-tagged Rim21, Dfg16, and Rim9. Rim21-HA was detected as a 68-kDa band on SDS-PAGE, which was shifted stepwise to lower molecular weights by sequential treatment with endoglycosidase H (Endo H) and  $\lambda$ -protein phosphatase ( $\lambda$ -PPase) (Fig. 1A). Thus, Rim21 undergoes post-translational glycosylation and phosphorylation. Dfg16-HA was detected as an

80-kDa band. Upon incubation with Endo H, the band was shifted to two faster migrating bands, of which the slower migrating band disappeared after  $\lambda$ -PPase treatment. Thus, like Rim21, Dfg16 is both glycosylated and phosphorylated. Rim9-HA was detected predominantly as a 33-kDa band along with a faint 29-kDa band. Endo-H treatment had no effect on these two bands, while incubation with  $\lambda$ -PPase caused a mobility shift of the 33-kDa band merging to the 29-kDa band. This suggested that Rim9 is a non-glycosylated phosphoprotein.

We then examined their cellular level in each deletion mutant after Endo-H treatment. Rim21-HA level was significantly reduced in *dfg16* $\Delta$  and *rim9* $\Delta$  mutant cells, particularly in *dfg16* $\Delta$  cells, indicating that Dfg16 and Rim9 are required for the maintenance of the cellular level of Rim21 (Fig. 1B). Rim9 also plays some role in maintaining Dfg16-HA, since Dfg16-HA level was slightly reduced in *rim9* $\Delta$  but not in *rim21* $\Delta$  cells. Both *rim21* $\Delta$  and *dfg16* $\Delta$  mutants had no effect on phosphorylated Rim9-HA level, but its non-phosphorylated form was increased. The results are indicative of that these proteins mutually influence their protein levels and phosphorylation status each other, implying their close interrelationship in the Rim101 pathway. The sites and functional significance of these phosphorylations are currently unknown and will be the subject of future investigations.

Given such close interrelationship, we further investigated their possible physical interactions. The interaction of Dfg16 with Rim21 and Rim9 was first examined by co-immunoprecipitation experiments using Dfg16-FLAG and anti-FLAG antibody. Rim21-HA and Rim9-HA were co-immunoprecipitated with Dfg16-FLAG with high and low efficiency, respectively (Fig. 1C). Next, Rim9-FLAG was used to study the interaction between Rim9 and Rim21. Rim21-HA was co-immunoprecipitated with Rim9-FLAG but with low efficiency. The observed low co-immunoprecipitation efficiency involving Rim9 might be a result of its dissociation in solubilized lysates. Almost identical results were obtained from alkaline-treated cells (Fig. S1). These findings suggest that Rim21, Dfg16 and Rim9 could form a pH-sensing complex in the Rim101 pathway.

***Rim21 and Dfg16 play distinct roles in the Rim101 pathway***– The functional relationship of Rim21 and Dfg16 is elusive at present. If one acts as the sensor subunit and the other acts regulatory, the

overexpression of the main component might bypass the requirement of the other. To test this possibility, the Rim101 pathway was monitored by the presence of proteolytically processed Rim101 in *rim21Δ dfg16Δ* double mutant cells after overexpression of either Rim21 or Dfg16. In alkaline-treated wild type (WT) cells, virtually all Rim101 was found in its processed form, indicative of the activation of the Rim101 pathway (Fig. 2). In *rim21Δ dfg16Δ* double mutants harboring empty vectors, the activation of the Rim101 pathway was totally abolished. Neither overexpression of Rim21 nor Dfg16 restored the activation of the Rim101 pathway. The Rim9 homolog PalI in *Aspergillus nidulans* is known to assist proper localization of the likely pH sensor PalH (22). Accordingly, Rim9 was co-overexpressed with either Rim21 or Dfg16, but the activation of the Rim101 pathway was still not restored. These results suggest that both Rim21 and Dfg16 possess distinct and indispensable roles in the Rim101 pathway.

*Rim21, Dfg16, and Rim9 localize to the plasma membrane in a patchy and mutually dependent manner*— Rim21, Dfg16, and Rim9 were C-terminally tagged with GFP by chromosomal fusion and their intracellular localization was examined at the endogenously-expressed level. Since the Rim21-GFP signal was very weak, Rim21 C-terminally tagged with two tandem GFPs (2xGFP) was expressed and monitored. The GFP-tagged proteins were detected in the plasma membrane and in some internal membrane structures reminiscent of the Golgi apparatus and the endosome (Fig. 3A). In the plasma membrane, they were not dispersed evenly but clustered in a patchy fashion. Their localization was significantly altered in each deletion mutant. In *rim21Δ* and *rim9Δ* cells, Dfg16-GFP was found in some intracellular compartments and mainly in the vacuolar membranes, respectively, but not in the plasma membranes. Likewise, Rim9-GFP accumulated mainly at intracellular punctuates reminiscent of the Golgi apparatus and the endosome, instead of at the plasma membranes, in *rim21Δ* and *dfg16Δ* cells. Rim21-2xGFP was not detected in most of either *dfg16Δ* or *rim9Δ* cells, probably due to its low protein level in these mutants (Fig. 1B). In some of *dfg16Δ* and *rim9Δ* cells, Rim21-2xGFP was found in intracellular organelles but not in the plasma membrane. These results indicate that localization of Rim21, Dfg16, and Rim9 to the plasma membrane is mutually dependent.

Given the patchy distribution of Rim21-, Dfg16-, and Rim9-GFP in the plasma membrane, one could imagine that these proteins localize to eisosomes on the plasma membrane. The eisosome is a recently discovered structure attached to the cytosolic face of the plasma membrane and distributed in a patchy manner (30). Pil1 is the main component of the eisosome, and required for the eisosome formation (30). Therefore, we tested the possibility by monitoring their co-localization with Pil1-mCherry. Only a small fraction of Dfg16- and Rim9-GFP co-localized with Pil1-mCherry (Fig. 3B). Alkaline treatment did not facilitate these co-localizations (Fig. S2). We then studied the distribution of Rim21-, Dfg16-, and Rim9-GFP in *pil1Δ* cells, in which eisosome proteins cannot localize in a patchy manner but accumulate in abnormal structures called eisosome remnants on the plasma membrane (30). All the proteins were detected at the plasma membrane in a patchy fashion as observed in WT cells (Fig. 3C). In addition, alkalization of *pil1Δ* cells activated the Rim101 pathway (Fig. 3D). These findings suggest that Rim21, Dfg16, and Rim9 are not constitutively localized to eisosomes and that the activation of the Rim101 pathway is independent of eisosomes.

*Rim21, Dfg16, and Rim9 are transported into the vacuole and degraded upon external alkalization*— The fate of Rim21, Dfg16, and Rim9 upon external alkalization (*e.g.*, their translocation into the cell and turnover) must be understood. First, their translocation was investigated. After 20 min of alkaline treatment, significant fractions of Rim21-2xGFP and Dfg16-/Rim9-GFP moved to the vacuolar lumen and intracellular punctuates reminiscent of the endosome (Fig. 4A). This observation suggests that they are internalized and transported to the vacuole upon alkalization.

Next, we examined the changes in the cellular levels of Rim21, Dfg16, and Rim9 by immunoblot analysis. Upon alkalization, the levels of Rim21-, Dfg16-, and Rim9-HA were decreased significantly (Fig. 4B). This finding, together with the above results, indicates that, upon alkalization, these proteins are internalized, transported into the vacuole, and degraded. After 120 min, a small amount of unphosphorylated Rim21-HA was detected, which was probably formed by *de novo* synthesis. This was confirmed by the absence of the corresponding band after alkaline treatment of Rim21-HA cells in the presence of cycloheximide, an inhibitor of *de novo* protein synthesis (Fig. 4B).

*Rim21 plays a central role in sensing alkaline pH*– Since Rim21, Dfg16, and Rim9 have a mutual influence on their cellular level and localization, it is difficult to examine the direct involvement of Rim21, Dfg16, and Rim9 in pH sensing using their respective deletion mutants. Consequently, we employed a transient protein degradation system called the auxin-inducible degron (AID) system (31) to selectively deplete each protein in the plasma membrane and examined its effect on the Rim101 pathway. In the AID system, proteins tagged with an AID-tag derived from a plant transcription factor are specifically degraded by a ubiquitin-proteasome system upon treatment with a phytohormone auxin (3-indoleacetic acid, IAA). The C-terminally tagged fusion protein Rim21-FLAG-AID, Dfg16-FLAG-AID, and Rim9-HA-AID were rapidly degraded to an undetectable level within 30 min after addition of IAA (Fig. 5). Accordingly, *RIM21-FLAG-AID*, *DFG16-FLAG-AID*, and *RIM9-HA-AID* cells were subjected to alkalization after pretreatment with IAA for 30 min. The activation of the Rim101 pathway was completely abolished in *RIM21-FLAG-AID* cells. In contrast, the activation was not altered in either *DFG16-FLAG-AID* or *RIM9-HA-AID* cells. In *RIM21-FLAG-AID* cells, without IAA treatment (mock), the Rim101 pathway was activated upon alkalization. Furthermore, Dfg16-HA and Rim9-HA in *RIM21-FLAG-AID* cells were not degraded by IAA treatment (Fig. S3). Based on these findings, we concluded that Rim21 is the pH-sensor molecule. Dfg16 and Rim9 seem to be involved indirectly in pH sensing through maintaining Rim21 level and, presumably, through assisting its plasma membrane localization.

*The C-terminal region of Rim21 is essential for activation of the Rim101 pathway*– The topology of the N- and C-termini of Rim21 was biochemically investigated to determine the region essential for pH sensing. Rim21 is predicted to span the membrane six and seven times by HMMTOP (<http://www.enzim.hu/hmmtop/>) and SOSUI (<http://bp.nuap.nagoya-u.ac.jp/sosui/>) programs, respectively. To analyze the topology of the N-terminus, a topological reporter protein, the mature portion of Suc2, was fused to the N-terminus of Rim21. The mature portion of Suc2 is rapidly N-glycosylated at multiple sites when translocated in the ER lumen, which is topologically equivalent to the extracellular side of the plasma membrane. This

system has been successfully applied to determine the topology of membrane proteins (27, 32). The Suc2-Rim21-FLAG fusion protein displayed, on SDS-PAGE, a slow-migrating band at 77 kDa in addition to a band with the predicted molecular weight (Fig. 6A). The additional band shifted down to the predicted band upon deglycosylation with Endo H, indicating that the fusion protein was glycosylated. Since Rim21 is a glycoprotein (Fig. 1A), Rim21-FLAG also showed a downshift on SDS-PAGE upon deglycosylation, but to a much lesser degree. This observation strongly suggests that the N-terminus of Rim21 is located in the extracellular space. The success of the AID tag experiment described above (Fig. 5) depends on the presence of the AID tag fused to the C-terminus of Rim21 in the cytosolic space (31). Thus, Rim21 seems to possess an odd number of transmembrane helices, probably seven, with its N- and C-termini facing the extracellular and cytosolic space, respectively.

Although Rim21 appears to have no regions showing similarity to known domains, one prominent feature of Rim21 is that the C-terminal cytosolic tail is rich in acidic amino acid residues. An estimated isoelectric point of the C-terminal tail region is 4.64 as opposed to 6.26 for the entire protein. A cluster of acidic amino acid residues (DEDDDENAEDEDDDE, *i.e.*, amino acid residues 496-511) is found near the C-terminus of Rim21. To examine a possible involvement of this acidic region in the Rim101 pathway, we engineered a Rim21 variant (Rim21ΔC) that lacks the most C-terminal region including the acidic cluster (amino acid residues 455-534). Cells expressing the Rim21ΔC did not activate the Rim101 pathway in response to external alkalization, indicating that this region is essential for the Rim101 pathway (Fig. 6B).

*Plasma membrane depolarization activates the Rim101 pathway*– External alkalization causes depolarization of the plasma membrane by collapsing proton electrochemical gradient across the plasma membrane. For this reason, we examined if plasma membrane depolarization alone, induced by a protonophore carbonyl cyanide *m*-chlorophenylhydrazone (CCCP), stimulates the Rim101 pathway without external alkalization. Upon CCCP treatment, the Rim101 pathway was activated in a Rim21-dependent manner (Fig. 7A). Thus, the CCCP-induced activation of the Rim101 pathway occurs through the sensor protein Rim21. Like external alkalization, CCCP treatment induced

internalization of Rim21, Dfg16, and Rim9 (Fig. S4A).

Besides proton electrochemical gradient, an asymmetric distribution of phospholipids, such as negatively-charged phosphatidylserine (PS), across the plasma membrane is known to be important for the membrane polarization (33). In the plasma membrane, PS is mostly confined to the inner leaflet resulting in its asymmetric distribution. We then studied the involvement of PS in regulation of the Rim101 pathway using *cho1Δ* cells that do not produce PS due to the missing PS synthase Cho1 (24, 34). In *cho1Δ* cells, the Rim101 pathway was constitutively activated even without alkaline treatment (Fig. 7B). The constitutive activation of the Rim101 pathway is also reported in *lem3Δ* cells (23). Lem3 is required for the asymmetric distribution of phospholipids in the plasma membrane. We confirmed the constitutive activation of the Rim101 pathway in *lem3Δ* cells. The activation level was comparable to that observed in *cho1Δ* cells (Fig. 7B). However, the activation efficiency was relatively low in both mutants as compared to in the alkaline-treated cells. Such low efficiency may arise from the presence of additional factors that contribute to membrane polarization in these mutants, including other phospholipids (*e.g.*, phosphatidylinositol and phosphoinositides) and proton electrochemical gradient. Internalization of Rim21-2xGFP and Dfg16-Rim9-GFP to intracellular organelles was also observed in *lem3Δ* cells, albeit at a low frequency (Fig. S4B). In *cho1Δ* cells, however, their internalization was difficult to be evaluated due to their weak signals for unknown reason (data not shown).

## DISCUSSION

In the present work, we have obtained some basic biochemical information of putative sensor molecules Rim21, Dfg16, and Rim9 concerning their localization, complex formation, and interrelationship. Such information could provide a base for future research into the molecular mechanisms of sensing extracellular pH and abnormal membrane lipid asymmetry.

Rim21 was found to act as the sensor molecule in the Rim101 pathway (Fig. 5). Then, the question is how Rim21 senses external alkalization and altered lipid asymmetry. We have shown that the Rim21-dependent activation of the Rim101 pathway, even without external alkalization, by the plasma membrane depolarization induced either by CCCP treatment (Fig. 7A) or by reduction of PS in the

inner leaflet of the plasma membrane (Fig. 7B). Thus, one possible hypothesis is that Rim21 senses external alkalization and altered lipid asymmetry by detecting depolarization of the plasma membrane. An alternative hypothesis is that Rim21 detects the reduction of negatively-charged lipids, such as PS, in the inner leaflet of the plasma membrane. The membrane depolarization caused by CCCP is reported to suppress almost completely the inward translocation of phospholipids across the membrane, *i.e.*, phospholipid flip (35, 36). Hence, the membrane depolarization by external alkalization may impair the phospholipid flip, thus leading to the reduction of PS in the inner leaflet of the plasma membrane. In this regard, it is significant that the C-terminal cytosolic region of Rim21, comprised of the acidic amino acid cluster, is required for the Rim101 pathway (Fig. 6B). Such highly acidic motif could play a critical role in the regulation of the Rim101 pathway since it generates a repulsive interaction with the negatively-charged lipids in the inner leaflet of the plasma membrane. Other hypotheses are also feasible. For example, the reduction in PS and the membrane depolarization may be simultaneously recognized by different regions of Rim21. In addition, the external alkalization and the altered lipid asymmetry may potentially cause the changes in the surface charge of the plasma membrane, which could then be sensed by Rim21. Certainly, more studies are needed.

At 120 min of alkaline treatment, Rim21-HA was *de novo* synthesized, whereas Dfg16-HA and Rim9-HA were not (Fig. 4B). The promoter region of *RIM21* contains two potential Nrg1-binding *cis*-elements (CCCCT and CCCTC). Nrg1 is a transcriptional repressor that negatively regulates expression of alkaline-responsive genes (5). In turn, the transcription of *NRG1* is directly repressed by Rim101 (5). Thus, activation of the Rim101 pathway leads to expression of genes that are usually repressed by Nrg1. Our result implicates that the Rim21 level is regulated, at least in part, by this positive feedback loop. In contrast, the level of Rim8, an arrestin-like protein essential for the Rim101 pathway, is regulated by a negative feedback loop, since the transcription of *RIM8* is directly repressed by Rim101 (5). It is therefore interesting to know if the Rim101 pathway is regulated elaborately by such positive and negative feedback loops.

Rim21, Dfg16, and Rim9 displayed a patchy rather than an even distribution in the plasma membrane. The assembly into such clusters may

facilitate the efficient transmission of signals of alkaline-pH and altered lipid asymmetry to downstream molecules. Immunoblot and microscopic analyses revealed that Rim21, Dfg16, Rim9 are internalized and degraded upon external alkalization (Fig. 4B). An important issue that should be addressed in the future is whether internalization of the sensor complex, as observed in

this work, is an essential process in transducing the signal of external alkalization or whether it is just an attenuation process of the Rim101 pathway. For this purpose, it would be necessary to monitor the Rim101 pathway in several endocytosis mutants with a highly-sensitive live imaging system to analyze the actions of these proteins and the downstream molecules at a single molecule level.

## REFERENCES

1. Peñalva, M. A. and Arst, H. N., Jr. (2002) Regulation of gene expression by ambient pH in filamentous fungi and yeasts. *Microbiol. Mol. Biol. Rev.* **66**, 426-446
2. Peñalva, M. A. and Arst, H. N., Jr. (2004) Recent advances in the characterization of ambient pH regulation of gene expression in filamentous fungi and yeasts. *Annu. Rev. Microbiol.* **58**, 425-451
3. Davis, D. A. (2009) How human pathogenic fungi sense and adapt to pH: the link to virulence. *Curr. Opin. Microbiol.* **12**, 365-370
4. Causton, H. C., Ren, B., Koh, S. S., Harbison, C. T., Kanin, E., Jennings, E. G., Lee, T. I., True, H. L., Lander, E. S., and Young, R. A. (2001) Remodeling of yeast genome expression in response to environmental changes. *Mol. Biol. Cell* **12**, 323-337
5. Lamb, T. M. and Mitchell, A. P. (2003) The transcription factor Rim101p governs ion tolerance and cell differentiation by direct repression of the regulatory genes *NRG1* and *SMP1* in *Saccharomyces cerevisiae*. *Mol. Cell. Biol.* **23**, 677-686
6. Lamb, T. M., Xu, W., Diamond, A., and Mitchell, A. P. (2001) Alkaline response genes of *Saccharomyces cerevisiae* and their relationship to the RIM101 pathway. *J. Biol. Chem.* **276**, 1850-1856
7. Serrano, R., Ruiz, A., Bernal, D., Chambers, J. R., and Ariño, J. (2002) The transcriptional response to alkaline pH in *Saccharomyces cerevisiae*: evidence for calcium-mediated signalling. *Mol. Microbiol.* **46**, 1319-1333
8. Barwell, K. J., Boysen, J. H., Xu, W., and Mitchell, A. P. (2005) Relationship of *DFG16* to the Rim101p pH response pathway in *Saccharomyces cerevisiae* and *Candida albicans*. *Eukaryot. Cell* **4**, 890-899
9. Li, W. and Mitchell, A. P. (1997) Proteolytic activation of Rim1p, a positive regulator of yeast sporulation and invasive growth. *Genetics* **145**, 63-73
10. Tréton, B., Blanchin-Roland, S., Lambert, M., Léplinge, A., and Gaillardin, C. (2000) Ambient pH signalling in ascomycetous yeasts involves homologues of the *Aspergillus nidulans* genes palF and palH. *Mol. Gen. Genet.* **263**, 505-513
11. Hayashi, M., Fukuzawa, T., Sorimachi, H., and Maeda, T. (2005) Constitutive activation of the pH-responsive Rim101 pathway in yeast mutants defective in late steps of the MVB/ESCRT pathway. *Mol. Cell. Biol.* **25**, 9478-9490
12. Lin, C. H., MacGurn, J. A., Chu, T., Stefan, C. J., and Emr, S. D. (2008) Arrestin-related ubiquitin-ligase adaptors regulate endocytosis and protein turnover at the cell surface. *Cell* **135**, 714-725
13. Shukla, A. K., Xiao, K., and Lefkowitz, R. J. (2011) Emerging paradigms of beta-arrestin-dependent seven transmembrane receptor signaling. *Trends Biochem. Sci.* **36**, 457-469
14. Henne, W. M., Buchkovich, N. J., and Emr, S. D. (2011) The ESCRT pathway. *Dev. Cell* **21**, 77-91
15. Xu, W., Smith, F. J., Jr., Subaran, R., and Mitchell, A. P. (2004) Multivesicular body-ESCRT components function in pH response regulation in *Saccharomyces cerevisiae* and *Candida albicans*. *Mol. Biol. Cell* **15**, 5528-5537
16. Babst, M., Katzmann, D. J., Estepa-Sabal, E. J., Meerloo, T., and Emr, S. D. (2002) Escrt-III: an endosome-associated heterooligomeric protein complex required for mvb sorting. *Dev. Cell* **3**, 271-282
17. Ito, T., Chiba, T., Ozawa, R., Yoshida, M., Hattori, M., and Sakaki, Y. (2001) A comprehensive two-hybrid analysis to explore the yeast protein interactome. *Proc. Natl. Acad. Sci. U.S.A.* **98**, 4569-4574
18. Xu, W. and Mitchell, A. P. (2001) Yeast PalA/AIP1/Alix homolog Rim20p associates with a PEST-like region and is required for its proteolytic cleavage. *J. Bacteriol.* **183**, 6917-6923
19. Weiss, P., Huppert, S., and Kölling, R. (2009) Analysis of the dual function of the ESCRT-III protein Snf7 in endocytic trafficking and in gene expression. *Biochem. J.* **424**, 89-97
20. Herranz, S., Rodríguez, J. M., Bussink, H. J., Sánchez-Ferrero, J. C., Arst, H. N., Jr., Peñalva, M. A., and Vincent, O. (2005) Arrestin-related proteins mediate pH signaling in fungi. *Proc. Natl. Acad. Sci. U.S.A.* **102**, 12141-12146
21. Negrete-Urtasun, S., Reiter, W., Diez, E., Denison, S. H., Tilburn, J., Espeso, E. A., Peñalva, M. A.,

- and Arst, H. N., Jr. (1999) Ambient pH signal transduction in *Aspergillus*: completion of gene characterization. *Mol. Microbiol.* **33**, 994-1003
22. Calcagno-Pizarelli, A. M., Negrete-Urtasun, S., Denison, S. H., Rudnicka, J. D., Bussink, H. J., Múnera-Huertas, T., Stanton, L., Hervás-Aguilar, A., Espeso, E. A., Tilburn, J., Arst, H. N., Jr., and Peñalva, M. A. (2007) Establishment of the ambient pH signaling complex in *Aspergillus nidulans*: PalI assists plasma membrane localization of PalH. *Eukaryot. Cell* **6**, 2365-2375
  23. Ikeda, M., Kihara, A., Denpoh, A., and Igarashi, Y. (2008) The Rim101 pathway is involved in Rsb1 expression induced by altered lipid asymmetry. *Mol. Biol. Cell* **19**, 1922-1931
  24. Hikiji, T., Miura, K., Kiyono, K., Shibuya, I., and Ohta, A. (1988) Disruption of the *CHO1* gene encoding phosphatidylserine synthase in *Saccharomyces cerevisiae*. *J. Biochem.* **104**, 894-900
  25. Longtine, M. S., McKenzie, A., 3rd, Demarini, D. J., Shah, N. G., Wach, A., Brachat, A., Philippsen, P., and Pringle, J. R. (1998) Additional modules for versatile and economical PCR-based gene deletion and modification in *Saccharomyces cerevisiae*. *Yeast* **14**, 953-961
  26. Sikorski, R. S. and Hieter, P. (1989) A system of shuttle vectors and yeast host strains designed for efficient manipulation of DNA in *Saccharomyces cerevisiae*. *Genetics* **122**, 19-27
  27. Kihara, A., Sakuraba, H., Ikeda, M., Denpoh, A., and Igarashi, Y. (2008) Membrane topology and essential amino acid residues of Phs1, a 3-hydroxyacyl-CoA dehydratase involved in very long-chain fatty acid elongation. *J. Biol. Chem.* **283**, 11199-11209
  28. Obara, K., Sekito, T., and Ohsumi, Y. (2006) Assortment of phosphatidylinositol 3-kinase complexes-Atg14p directs association of complex I to the pre-autophagosomal structure in *Saccharomyces cerevisiae*. *Mol. Biol. Cell* **17**, 1527-1539
  29. Yamagata, M., Obara, K., and Kihara, A. (2011) Sphingolipid synthesis is involved in autophagy in *Saccharomyces cerevisiae*. *Biochem. Biophys. Res. Commun.* **410**, 786-791
  30. Walther, T. C., Brickner, J. H., Aguilar, P. S., Bernales, S., Pantoja, C., and Walter, P. (2006) Eisosomes mark static sites of endocytosis. *Nature* **439**, 998-1003
  31. Nishimura, K., Fukagawa, T., Takisawa, H., Kakimoto, T., and Kanemaki, M. (2009) An auxin-based degron system for the rapid depletion of proteins in nonplant cells. *Nat. Methods* **6**, 917-922
  32. Han, G., Gable, K., Yan, L., Natarajan, M., Krishnamurthy, J., Gupta, S. D., Borovitskaya, A., Harmon, J. M., and Dunn, T. M. (2004) The topology of the Lcb1p subunit of yeast serine palmitoyltransferase. *J. Biol. Chem.* **279**, 53707-53716
  33. Gurtovenko, A. A. and Vattulainen, I. (2008) Membrane potential and electrostatics of phospholipid bilayers with asymmetric transmembrane distribution of anionic lipids. *J. Phys. Chem. B* **112**, 4629-4634
  34. Letts, V. A., Klig, L. S., Bae-Lee, M., Carman, G. M., and Henry, S. A. (1983) Isolation of the yeast structural gene for the membrane-associated enzyme phosphatidylserine synthase. *Proc. Natl. Acad. Sci. U.S.A.* **80**, 7279-7283
  35. Hanson, P. K. and Nichols, J. W. (2001) Energy-dependent flip of fluorescence-labeled phospholipids is regulated by nutrient starvation and transcription factors, *PDR1* and *PDR3*. *J. Biol. Chem.* **276**, 9861-9867
  36. Stevens, H. C. and Nichols, J. W. (2007) The proton electrochemical gradient across the plasma membrane of yeast is necessary for phospholipid flip. *J. Biol. Chem.* **282**, 17563-17567
  37. Robinson, J. S., Klionsky, D. J., Banta, L. M., and Emr, S. D. (1988) Protein sorting in *Saccharomyces cerevisiae*: isolation of mutants defective in the delivery and processing of multiple vacuolar hydrolases. *Mol. Cell. Biol.* **8**, 4936-4948

*Acknowledgements*—We thank Dr. T. Maeda (Institute of Molecular and Cellular Biosciences, University of Tokyo, Japan) for providing a plasmid for expression of HA-Rim101 (pF11). The yeast strain for the AID system (BY25598) was provided by the National Bio-Resource Project (NBRP) of the MEXT, Japan. We are grateful to Dr. T. Toyokuni for editing the manuscript.

## FOOTNOTES

\*This work was supported by a Grant-in-Aid for Young Scientists (B) (23770135) to KO and a Grant-in-Aid for Challenging Exploratory Research (23657120) to AK from the Japan Society for the Promotion of Science (JSPS). This work was also supported by The Naito Foundation Subsidy for Promotion of Specific Research Projects to KO from The Naito Foundation.

<sup>1</sup>To whom correspondence may be addressed: Faculty of Pharmaceutical Sciences, Hokkaido University, Kita 12-jo Nishi 6-chome, Kita-ku, Sapporo, 060-0812, Japan, Tel.: +81-11-706-3754; Fax: +81-11-706-4900; E-mail: kihara@pharm.hokudai.ac.jp

<sup>2</sup>Frontier Research Center, Tokyo Institute of Technology, S2-12, 4259 Nagatsuda, Midori-ku, Yokohama, 226-8503, Japan

<sup>3</sup>The abbreviations used are: ESCRT, endosomal sorting complex required for transport; SD, synthetic dextrose; IAA, 3-indoleacetic acid; PS, phosphatidylserine; PE, phosphatidylethanolamine; CCCP, carbonyl cyanide *m*-chlorophenylhydrazone;  $\lambda$ -PPase,  $\lambda$ -protein phosphatase; PMSF, phenylmethylsulphonyl fluoride; Eondo H, endoglycosidase H; WT, wild type; AID, auxin-inducible degra

## FIGURE LEGENDS

**FIGURE 1. Rim21, Dfg16 and Rim9 are mutually dependent in the Rim101 pathway.** A. Total lysates were prepared from YOK2027 (*rim21* $\Delta$ ), YOK2054 (*dfg16* $\Delta$ ), and YOK2055 (*rim9* $\Delta$ ) cells harboring pOK313 (*RIM21-HA*), pOK314 (*DFG16-HA*), and pOK318 (*RIM9-HA*), respectively, and treated with or without Endo H and  $\lambda$ -PPase. Immunoblotting was performed with anti-HA antibody. Arrows, Dfg16-HA; asterisks, non-specific bands. B. Total lysates were prepared from the following cells: YOK2027 (*rim21* $\Delta$ ), YOK2095 (*rim21* $\Delta$  *dfg16* $\Delta$ ), and YOK2095 (*rim21* $\Delta$  *rim9* $\Delta$ ) cells containing pOK313 (*RIM21-HA*); YOK2054 (*dfg16* $\Delta$ ), YOK2095 (*rim21* $\Delta$  *dfg16* $\Delta$ ), and YOK2097 (*dfg16* $\Delta$  *rim9* $\Delta$ ) cells containing pOK314 (*DFG16-HA*); and YOK2055 (*rim9* $\Delta$ ), YOK2095 (*rim21* $\Delta$  *rim9* $\Delta$ ), and YOK2097 (*dfg16* $\Delta$  *rim9* $\Delta$ ) cells containing pOK318 (*RIM9-HA*). After Endo-H treatment, immunoblotting was performed with anti-HA antibody or, to demonstrate uniform protein loading, with anti-Pgk1 antibody. C. Total lysates were prepared from YOK2540 (*RIM21-HA*), YOK2546 (*RIM21-HA DFG16-FLAG*), YOK2547 (*RIM21-HA RIM9-FLAG*), YOK2542 (*RIM9-HA*), and YOK2548 (*RIM9-HA DFG16-FLAG*) cells. Immunoblotting of co-precipitated proteins with anti-FLAG M2-agarose were performed with anti-HA and anti-FLAG antibodies. IB, immunoblot; IP, immunoprecipitation; arrowheads, co-immunoprecipitates; asterisks, non-specific bands.

**FIGURE 2. The functions of Rim21 and Dfg16 are irreplaceable by each other in the Rim101 pathway.** After 20-min alkaline treatment, total lysates were prepared from SEY6210 (WT) and YOK2095 (*rim21* $\Delta$  *dfg16* $\Delta$ ) cells harboring pF11 (*HA-RIM101*) and empty vectors (pRS423 and pRS424) with the indicated combination of plasmids for overexpression of Rim21-HA (pOK315 or pOK328), Dfg16-FLAG (pOK330), and Rim9-HA (pOK320). After Endo-H treatment, immunoblotting was performed with anti-HA and anti-FLAG antibodies or, to demonstrate uniform protein loading, with anti-Pgk1 antibody. FL, full-length;  $\Delta$ C, Rim101 $\Delta$ C.

**FIGURE 3. Rim21, Dfg16, and Rim9 are localized to the plasma membrane in a patchy and mutually dependent manner.** A. YOK3208 (*RIM21-2xEGFP*), YOK3209 (*RIM21-2xEGFP dfg16* $\Delta$ ), YOK3210 (*RIM21-2xEGFP rim9* $\Delta$ ), YOK2210 (*DFG16-EGFP*), YOK2211 (*DFG16-EGFP rim21* $\Delta$ ), YOK2212 (*DFG16-EGFP rim9* $\Delta$ ), YOK2229 (*RIM9-EGFP*), YOK2215 (*RIM9-EGFP rim21* $\Delta$ ), and YOK2216 (*RIM9-EGFP dfg16* $\Delta$ ) cells were subjected to fluorescence microscopy. Bar, 5  $\mu$ m. B. YOK2729 (*DFG16-EGFP PIL1-mCherry*) and YOK2731 (*RIM9-EGFP PIL1-mCherry*) cells were subjected to fluorescence microscopy. Arrows, Dfg16-EGFP or Rim9-EGFP that co-localized with Pill1-mCherry;

arrowheads, Dfg16-EGFP or Rim9-EGFP that did not co-localize with Pil1-mCherry; bar, 5  $\mu$ m. C. YOK2743 (*RIM21-EGFP pil1* $\Delta$ ), YOK2744 (*DFG16-EGFP pil1* $\Delta$ ), and YOK2745 (*RIM9-EGFP pil1* $\Delta$ ) cells were subjected to fluorescence microscopy. Bar, 5  $\mu$ m. D. YOK2027 (*rim21* $\Delta$ ), YOK2210 (*DFG16-EGFP*), and YOK2744 (*DFG16-EGFP pil1* $\Delta$ ) cells harboring pFI1 (*HA-RIM101*) were collected after 20-min alkaline treatment. Immunoblotting was performed with anti-HA antibody. FL, full-length;  $\Delta$ C, Rim101 $\Delta$ C.

**FIGURE 4. Rim21, Dfg16, and Rim9 are degraded upon external alkalization.** A. Before and after 20-min alkaline treatment, YOK3208 (*RIM21-2xEGFP*), YOK2210 (*DFG16-EGFP*), and YOK2229 (*RIM9-EGFP*) cells were subjected to fluorescence microscopy. Bar, 5  $\mu$ m. B. Total lysates were prepared from YOK2559 (*RIM21-HA*), YOK2560 (*DFG16-HA*), and YOK2561 (*RIM9-HA*) cells. After Endo-H treatment, immunoblotting was performed with anti-HA or, to demonstrate uniform protein loading, with anti-Pgk1 antibody. CHX, cycloheximide

**FIGURE 5. Rim21 is the sensor protein in the Rim101 pathway.** YOK2848 (*RIM21-FLAG-AID*), YOK2849 (*DFG16-FLAG-AID*), and YOK2846 (*RIM9-HA-AID*) cells harboring pFI1 (*HA-RIM101*) were pretreated with 500  $\mu$ M IAA or ethanol (mock) for 30 min. Before or after 20-min alkaline treatment, followed by Endo-H treatment, immunoblotting was performed with anti-HA and anti-FLAG antibodies or, to demonstrate uniform protein loading, with anti-Pgk1 antibody. FL, full-length;  $\Delta$ C, Rim101 $\Delta$ C; asterisk, non-specific band.

**FIGURE 6. The acidic motif of Rim21 is involved in the regulation of the Rim101 pathway.** A. Total lysates were prepared from YOK2027 (*rim21* $\Delta$ ) cells harboring pOK311 (*RIM21-FLAG*) or pOK387 (*SUC2-RIM21-FLAG*) cells and treated with or without Endo H. Immunoblotting was performed with anti-FLAG antibody. Arrowhead, Suc2-Rim21-FLAG glycosylated at the Suc2 moiety. B. Total lysates were prepared from SEY6210 (WT) and YOK2027 (*rim21* $\Delta$ ) cells harboring pFI1 (*HA-RIM101*) together with pRS313 (empty vector), pOK313 (*RIM21-HA*), or pOK419 (*RIM21* $\Delta$ C-HA). After Endo-H treatment, immunoblotting was performed with anti-HA antibody or, to demonstrate uniform protein loading, with anti-Pgk1 antibody. FL, full-length;  $\Delta$ C, Rim101 $\Delta$ C; arrowheads, Rim21 variants; asterisk, non-specific band.

**FIGURE 7. Plasma membrane depolarization activates the Rim101 pathway.**

A. SEY6210 (WT) and YOK2098 (*rim21* $\Delta$ ) cells harboring pFI1 (*HA-RIM101*) were grown at pH 5.5 and treated with CCCP or ethanol (mock) for 20 min. Immunoblotting was performed with anti-HA antibody or, to demonstrate uniform protein loading, with anti-Pgk1 antibody. B. Total lysates were prepared from KCY662 (WT), YOK2098 (*rim21* $\Delta$ ), KCY692 (*lem3* $\Delta$ ), and KCY1113 (*cho1* $\Delta$ ) cells grown in the presence of 1 mM ethanolamine. Immunoblotting was performed with anti-HA antibody or, to demonstrate uniform protein loading, with anti-Pgk1 antibody. FL, full-length;  $\Delta$ C, Rim101 $\Delta$ C.

**TABLE 1.** Yeast strains used in this study

Strain	Genotype	Source
SEY6210	<i>MAT<math>\alpha</math> his3 leu2 ura3 trp1 lys2 suc2</i>	(37)
YOK2027	SEY6210, <i>rim21<math>\Delta</math>::KanMX4</i>	This study
YOK2053	SEY6210, <i>rim21<math>\Delta</math>::NatNT2</i>	This study
YOK2054	SEY6210, <i>dfg16<math>\Delta</math>::NatNT2</i>	This study
YOK2055	SEY6210, <i>rim9<math>\Delta</math>::NatNT2</i>	This study
YOK2095	SEY6210, <i>rim21<math>\Delta</math>::NatNT2 dfg16<math>\Delta</math>::KanMX4</i>	This study
YOK2096	SEY6210, <i>rim21<math>\Delta</math>::NatNT2 rim9<math>\Delta</math>::KanMX4</i>	This study
YOK2097	SEY6210, <i>dfg16<math>\Delta</math>::NatNT2 rim9<math>\Delta</math>::KanMX4</i>	This study
YOK3208	SEY6210, <i>RIM21-2xEGFP::KanMX6</i>	This study
YOK3209	SEY6210, <i>RIM21-2xEGFP::KanMX6 dfg16<math>\Delta</math>::NatNT2</i>	This study
YOK3210	SEY6210, <i>RIM21-2xEGFP::KanMX6 rim9<math>\Delta</math>::NatNT2</i>	This study
YOK3211	SEY6210, <i>RIM21-2xEGFP::KanMX6 lem3<math>\Delta</math>::NatNT2</i>	This study
YOK2743	SEY6210, <i>RIM21-EGFP::NatNT2 pil1<math>\Delta</math>::KanMX4</i>	This study
YOK2210	SEY6210, <i>DFG16-EGFP::NatNT2</i>	This study
YOK2211	SEY6210, <i>DFG16-EGFP::NatNT2 rim21<math>\Delta</math>::KanMX4</i>	This study
YOK2212	SEY6210, <i>DFG16-EGFP::NatNT2 rim9<math>\Delta</math>::KanMX4</i>	This study
YOK2214	SEY6210, <i>DFG16-EGFP::NatNT2 lem3<math>\Delta</math>::KanMX4</i>	This study
YOK2744	SEY6210, <i>DFG16-EGFP::NatNT2 pil1<math>\Delta</math>::KanMX4</i>	This study
YOK2729	SEY6210, <i>DFG16-EGFP::NatNT2 PIL1-mChery::KanMX6</i>	This study
YOK2229	SEY6210, <i>RIM9-EGFP::NatNT2</i>	This study
YOK2215	SEY6210, <i>RIM9-EGFP::NatNT2 rim21<math>\Delta</math>::KanMX4</i>	This study
YOK2216	SEY6210, <i>RIM9-EGFP::NatNT2 dfg16<math>\Delta</math>::KanMX4</i>	This study
YOK2218	SEY6210, <i>RIM9-EGFP::NatNT2 lem3<math>\Delta</math>::KanMX4</i>	This study
YOK2745	SEY6210, <i>RIM9-EGFP::NatNT2 pil1<math>\Delta</math>::KanMX4</i>	This study
YOK2731	SEY6210, <i>RIM9-EGFP::NatNT2 PIL1-mChery::KanMX6</i>	This study
YOK2559	SEY6210, <i>RIM21-HA::KanMX6</i>	This study
YOK2560	SEY6210, <i>DFG16-HA::KanMX6</i>	This study
YOK2561	SEY6210, <i>RIM9-HA::KanMX6</i>	This study
YOK2540	SEY6210, <i>pep4<math>\Delta</math>::LEU2 prb1<math>\Delta</math>::NatNT2 RIM21-HA::TRP1</i>	This study
YOK2546	SEY6210, <i>pep4<math>\Delta</math>::LEU2 prb1<math>\Delta</math>::NatNT2 RIM21-HA::TRP1 DFG16-FLAG::KanMX6</i>	This study
YOK2547	SEY6210, <i>pep4<math>\Delta</math>::LEU2 prb1<math>\Delta</math>::NatNT2 RIM21-HA::TRP1 RIM9-FLAG::KanMX6</i>	This study
YOK2542	SEY6210, <i>pep4<math>\Delta</math>::LEU2 prb1<math>\Delta</math>::NatNT2 RIM9-HA::TRP1</i>	This study
YOK2548	SEY6210, <i>pep4<math>\Delta</math>::LEU2 prb1<math>\Delta</math>::NatNT2 RIM9-HA::TRP DFG16-FLAG::KanMX6</i>	This study

KCY662	SEY6210, <i>RSB1-HA::TRP1</i>	(23)
YOK2098	SEY6210, <i>RSB1-HA::TRP1 rim21Δ::KanMX4</i>	This study
KCY692	SEY6210, <i>RSB1-HA::TRP1 lem3Δ::HIS3</i>	(23)
KCY1113	SEY6210, <i>RSB1-HA::TRP1 cho1Δ::KanMX4</i>	This study
YOK2541	SEY6210, <i>pep4Δ::LEU2 prb1Δ::NatNT2 DFG16-HA::TRP1</i>	This study
YOK2738	SEY6210, <i>pep4Δ::LEU2 prb1Δ::NatNT2 DFG16-HA::TRP1</i> <i>RIM21-FLAG::KanMX6</i>	This study
YOK2739	SEY6210, <i>pep4Δ::LEU2 prb1Δ::NatNT2 DFG16-HA::TRP1</i> <i>RIM21(13R)-FLAG::KanMX6</i>	This study
BY25598	<i>MATa his3 leu2 ura3 trp1 ade2 can1 P<sub>ADH</sub>-OsTIR1-Myc::URA3</i>	(31)
YOK2848	BY25598, <i>RIM21-FLAG-AID::KanMX6</i>	This study
YOK2891	BY25598, <i>RIM21-FLAG-AID::KanMX6 DFG16-HA::TRP1</i>	This study
YOK2892	BY25598, <i>RIM21-FLAG-AID::KanMX6 RIM9-HA::TRP1</i>	This study
YOK2849	BY25598, <i>DFG16-FLAG-AID::KanMX6</i>	This study
YOK2846	BY25598, <i>RIM9-HA-AID::KanMX6</i>	This study

---

Figure.1

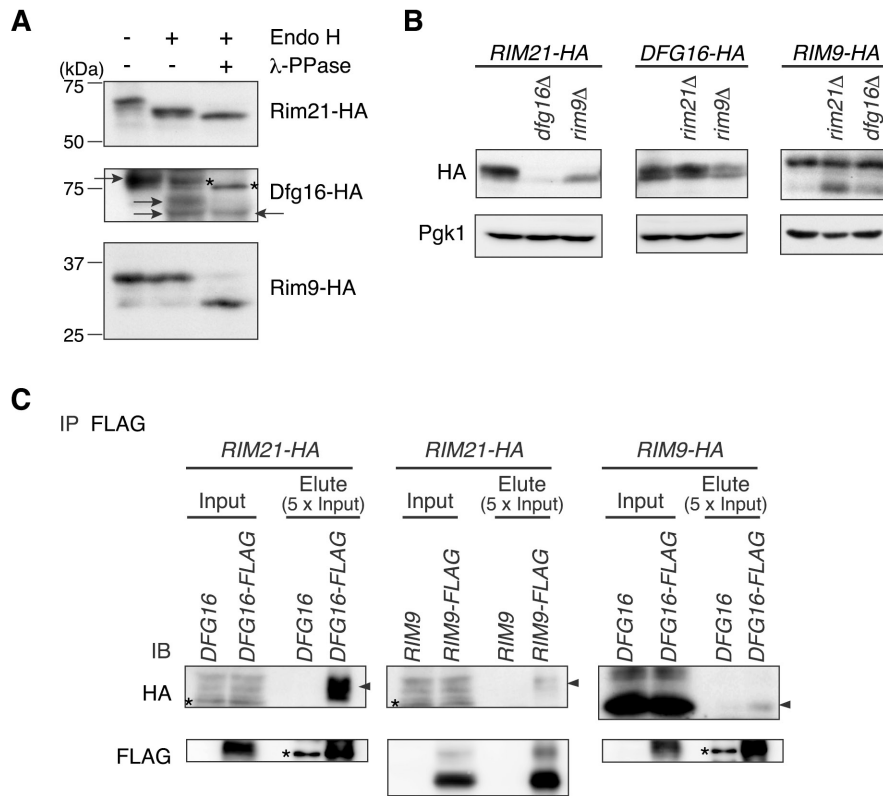


Figure 2

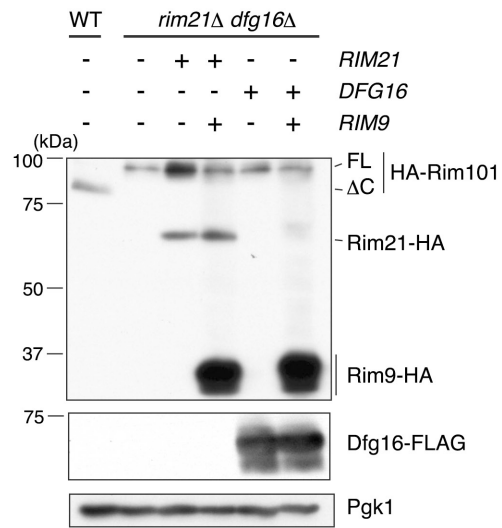


Figure 3

*Rim21 is the sensor protein that detects ambient pH*

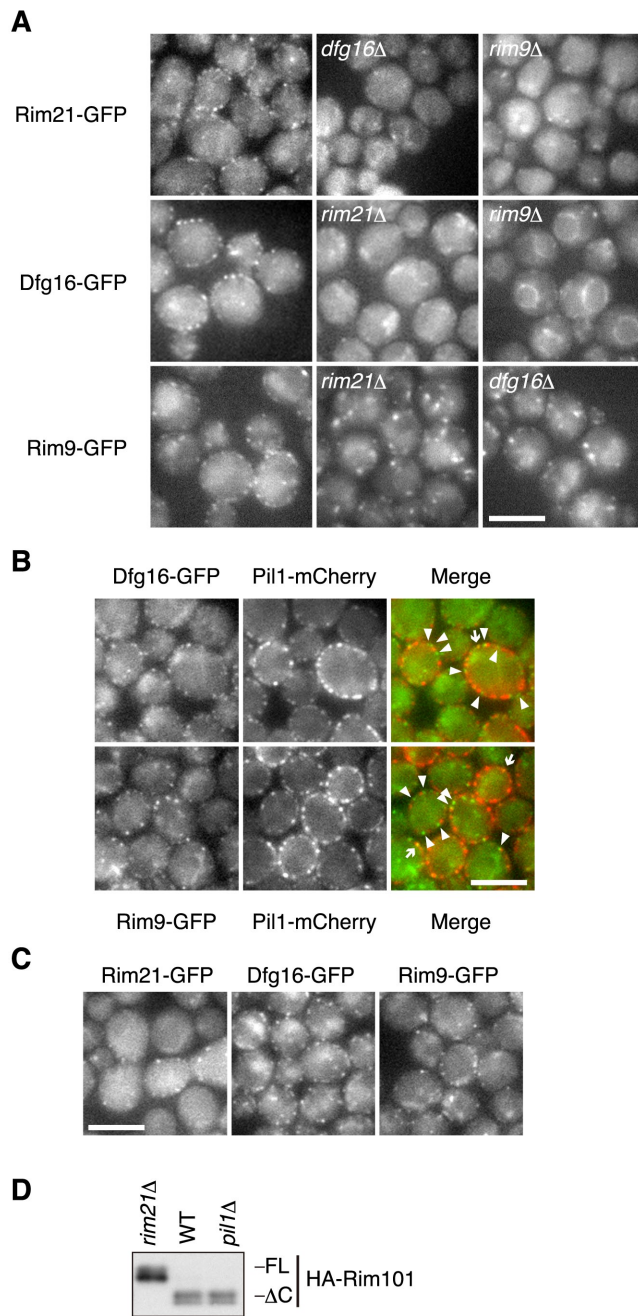


Figure 4

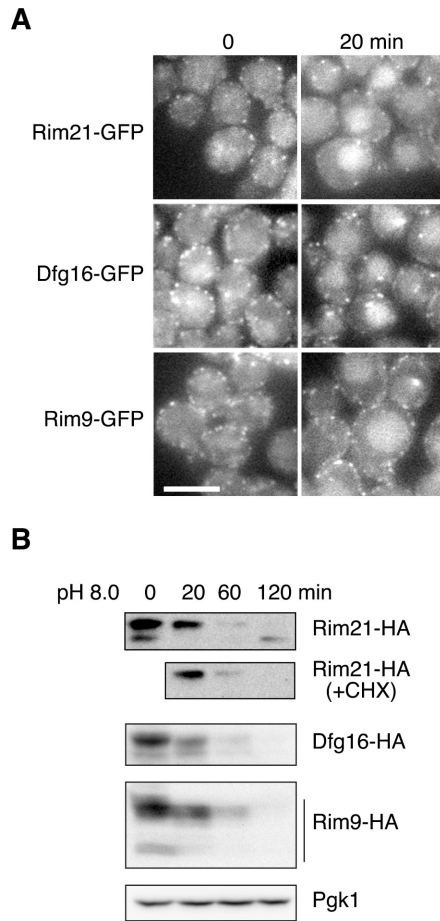


Figure 5

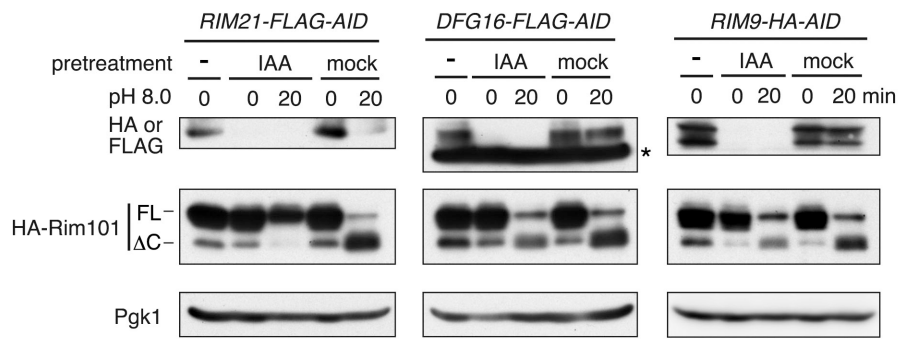


Figure 6

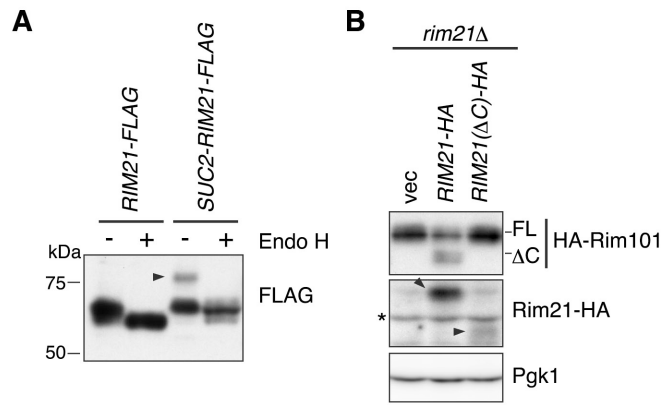


Figure 7

